Excitation of a higher order transverse mode in an optically pumped $In_{0.15}Ga_{0.85}N/In_{0.05}Ga_{0.95}N$ multiquantum well laser structure

Daniel Hofstetter,[a] David P. Bour, Robert L. Thornton, and N. M. Johnson
Xerox Palo Alto Research Center, Palo Alto, California 94304

We report a comparison between measured and calculated far field data for an optically pumped $In_{0.15}Ga_{0.85}N/In_{0.05}Ga_{0.95}N$ multiquantum well laser structure with AlGaN cladding layers. Optical pumping of the semiconductor device was performed with a pulsed 337 nm N_2 laser, whose beam was focused to a narrow stripe. A thin upper cladding layer allowed efficient pumping of the $In_{0.15}Ga_{0.85}N/In_{0.05}Ga_{0.95}N$ laser structure. Despite high distributed cavity losses of at least 30 cm^{-1}, and although gain occurred in the small active region only, the seventh order transverse mode was supported in a waveguide formed by the entire 5-μm-thick epitaxial layer structure. Excellent agreement is demonstrated between measured and calculated far field patterns of the lasing mode.

There is considerable interest in applications of blue semiconductor lasers fabricated in the III–V nitrides. The use of compact short wavelength light sources will improve the resolution of scanners and printers as well as increase the storage density of optical disks. High quality GaN films and AlGaInN heterostructures can be grown epitaxially in organometallic vapor phase epitaxy (OMVPE) reactors as was described earlier.[1–4] Prior to the fabrication of injection lasers it is possible to achieve stimulated light emission of the grown material by optical pumping.[5–8]

We report in this letter the optical excitation of a higher order lasing mode which propagates in a multimode waveguide formed by the entire 5-μm-thick epitaxial layer stack with the sapphire substrate providing the lower cladding layer. Since observations of a threshold in the output versus pump intensity characteristic, TE polarization of the emission, and linewidth narrowing above threshold are necessary but not sufficient conditions to conclude lasing, we include here for the first time, to the best of our knowledge, a comprehensive investigation of the transverse far field pattern to demonstrate lasing under photopumping conditions. Similar measurements on GaAs/AlGaAs injection lasers have been made earlier, but their main goal was to give a proof of existence of Hermite–Gaussian mode patterns in semiconductor light sources.[9,10] A near field calculation using the effective index method reveals that the seventh order mode of this thick multimode waveguide has maximum overlap with the multiple quantum well (MQW) structure in the center of the active region. Further calculations show an excellent agreement of the measured and the calculated far field pattern for this mode.

For these experiments, we used *C*-face sapphire (Al_2O_3) wafers as the substrate material. Growth was performed in an OMVPE system. On the sapphire, we grew 4 μm of GaN, followed by a 500-nm-thick $Al_{0.1}Ga_{0.9}N$ lower cladding layer, a 240-nm-thick GaN/InGaN waveguide, and a 50-nm-thick $Al_{0.1}Ga_{0.9}N$ upper cladding layer. Because of the relatively low carrier diffusion length in nitride films, the thin upper cladding layer was required for optical pumping of the MQWs. The active region consisted of five 25-Å-wide $In_{0.15}Ga_{0.85}N$ QWs separated by 70-Å-thick $In_{0.05}Ga_{0.95}N$ barrier layers. This MQW stack was sandwiched between two 100-nm-thick GaN waveguide layers.

The processing of the 2-mm-long laser bars was straightforward and included sawing of 2.2-mm-long and 10-mm-wide pieces, subsequent polishing of both facets, and high reflection (HR) coating of one facet. For this purpose, we used five pairs of $\lambda/4$ thick SiO_2/TiO_2 layers with a final reflectance of more than 90%. Since the optical output from the HR-coated facet was only 5% compared to that of the uncoated one, we used the latter for the succeeding measurements.

Optical pumping was carried out using a pulsed 337 nm N_2 laser ($r_{\text{pulse}}=5$ Hz, $P_{\text{peak}}=250$ kW, $W_{\text{pulse}}=75$ μJ) whose light was focused to a 100-μm-wide and approximately 4-mm-long stripe using both a spherical and a cylindrical lens. In order to attenuate the pump intensity, we inserted an increasing number of 1-mm-thick glass slides into the pump beam; these glass plates acted as neutral density filters for the ultraviolet (UV) emission of the nitrogen laser (optical density $\sim$0.05 per slide). The output intensity of the semiconductor laser was collected by an optical multimode fiber and fed into a grating spectrometer ($\Lambda=1200$ lines/mm, $d_{\text{focus}}=0.1$ m). The latter allowed simultaneous measurement of the laser spectrum and the output intensity. Although the spectral resolution of the spectrometer was only around 1 nm and therefore not sufficient to see single Fabry–Pérot modes in the laser spectrum, we used this spectrometer for determination of the linewidth of the blue laser emission.

The measurement of the far field was accomplished by placing a charge coupled device (CCD) camera without an objective lens in front of the laser facet. The distance between the laser and camera was chosen to be well outside the Rayleigh range for our 5-μm-wide aperture ($d_{\text{Rayleigh}}=2$ mm), but was chosen also to give maximal picture size of the far field intensity distribution on the camera.

Figure 1 shows the output intensity and the linewidth as a function of the nitrogen laser pump intensity; the threshold intensity is at 0.16 a.u. An investigation of the threshold intensities and the differential quantum efficiencies of devices with cleaved, polished, uncoated, and coated facets showed no significant differences between them, indicating

[a]Electronic mail: hofstetter@parc.xerox.com

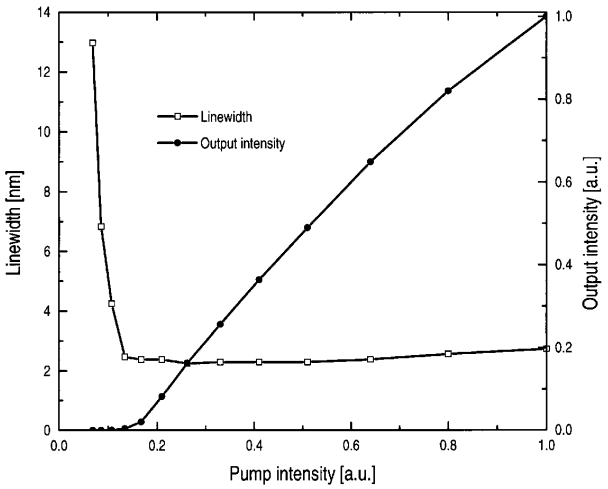

FIG. 1. Laser output intensity and linewidth vs pump intensity for a 2-mm-long bar pumped with a pulsed 337 nm nitrogen laser.

very high distributed cavity losses. These losses may be associated with the high defect density of the films, or the even higher defect density[11] near the interface between the 4-μm-thick GaN layer, in which part of the lasing mode is localized, and the sapphire substrate.

According to Fig. 1, we measured typical subthreshold linewidths of 15 nm, whereas the linewidth above threshold was on the order of 2 nm. The polarization state of the blue laser emission (λ-410 nm) was TE, exceeding the fraction of TM-polarized light by a factor of 50. Below threshold, no polarization effect was seen.

The far field below threshold exhibited no interference features and measured approximately 50°×25° (first value: $\perp$ to epitaxial layers). Above threshold, the far field angle in the direction parallel to the epitaxial layers collapsed to below 10°; in the other direction, we could see several intensity maxima and minima, as shown by the solid line of Fig. 2. In addition, two bright intensity spots occurred at angles of $\pm$18° off the optical axis. These features indicate that our

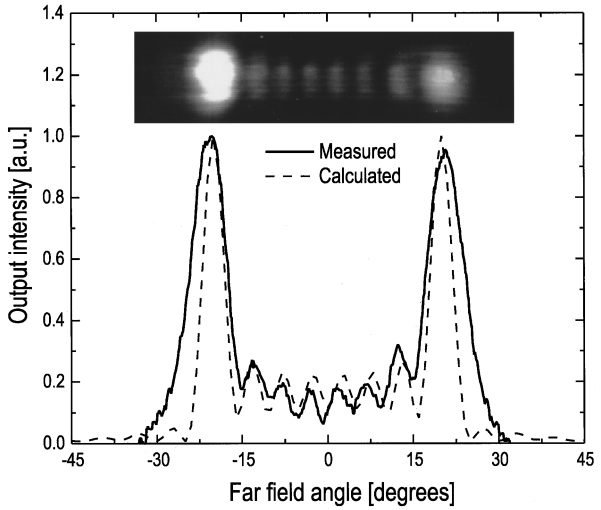

FIG. 2. Comparison between measured (solid) and calculated (dotted) far field patterns of the test device in the direction perpendicular to the epitaxial layer plane. The inset shows a CCD image of the measured far field distribution.

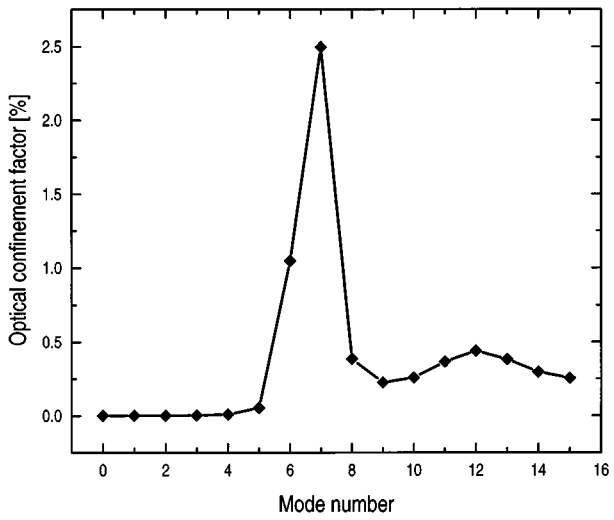

FIG. 3. Calculated confinement factors for different lasing modes. The seventh order mode of the multimode waveguide has maximum overlap with the MQW structure.

devices oscillate in a higher order transverse mode of the entire 5-μm-thick epitaxial layer stack, with air and sapphire as the upper and lower cladding layers, respectively. This mode, however, also overlaps well with the zero order mode of the 240-nm-thick GaN/InGaN waveguide, with air and AlGaN as the cladding layers.

The calculations presented below were performed with a dedicated program[12] and used refractive index values of $n_{\text{sapphire}}=1.766$, $n_{\text{GaN}}=2.51$, $n_{\text{AlGaN}}=2.48$, and $n_{\text{InGaN}}=2.56$, where n_{InGaN} represents an average number for the MQW/barrier layer stack.[13] The calculation of the confinement factors between the lasing modes and the MQW structure resulted in small values of below 0.1% for mode numbers 0–5 and also for most of mode numbers 8–15. For mode numbers 6 and 7, we calculated higher values of 1.1% and 2.5%, respectively. This surprising results is plotted in Fig. 3. The reason for the high overlap value of especially the seventh order mode is a result of the high index steps at the AlGaN/air and the GaN/sapphire interfaces. These index steps define a 5-μm-thick multimode waveguide in which the shape of the seventh order mode happens to nearly coincide with the zero order mode of the asymmetric 240-nm-thick GaN/InGaN waveguide. The same effect also increases the confinement factors of some even higher order modes (mode numbers 10–12) to values substantially above 0. As a comparison, we also calculated the confinement factor for the zero order mode of a 240-nm-thick GaN/InGaN waveguide with symmetric and semi-infinite AlGaN cladding layers. The value obtained for this case (3.8%) was slightly higher than the one for the best overlapping mode of the above asymmetric configuration.

The calculated near field distribution of the seventh order mode mentioned above (see Fig. 4) is very similar to the zero order mode of the GaN/InGaN waveguide. However, since the top and bottom AlGaN layers are thin, a significant energy fraction from the zero order mode radiates into the 4-μm-thick GaN layer. Optical losses in this layer are sufficiently low, however, that a well confined optical mode is established in the waveguide with the sapphire substrate as

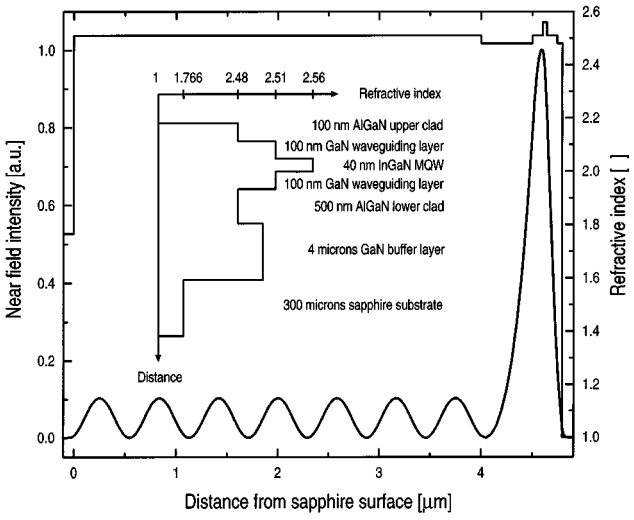

FIG. 4. Calculated near field distribution and corresponding refractive indices for the test device in the direction perpendicular to the epitaxial layer plane. The layer structure with the corresponding refractive indices is shown in the inset (not to scale).

the lower cladding layer. Among the modes of this much thicker multimode waveguide, the seventh order mode, as calculated, provides the greatest overlap with the quantum wells.

The dotted line of Fig. 2 corresponds to the calculated far field of this seventh order mode. The angle between the two most intense emission lobes in the direction perpendicular to the epitaxial layers is 36°. This angle, the relative heights of the different intensity peaks, their angular distribution, and also their modulation depth show excellent agreement with the measured far field pattern which is represented by the solid line of Fig. 2.

In summary, we have shown lasing action in an optically pumped $In_{0.15}Ga_{0.85}N/In_{0.05}Ga_{0.95}N$ MQW laser structure. This first comprehensive study of the far field of such devices exhibited two bright intensity spots at angles of $\pm 18°$ indicating emission from a 5-μm-wide aperture that is formed by all epitaxial layers on top of the sapphire substrate. As could be shown by calculations of the confinement factors, the propagating mode in this multimode waveguide was the seventh order mode. The propagation of this mode was associated with very high distributed losses in the cavity; this fact was confirmed by the observation that the threshold intensity was nearly independent of the facet mirror quality. By assuming that the mirror loss of uncoated facets is only a small fraction of the internal distributed cavity loss, we can place a lower limit on the internal loss of 30 cm^{-1}. For a symmetric waveguide, we would expect less optical penetration into the thick GaN layer, and hence lower loss. However, these results indicate that even a symmetric waveguide with the above compositions and with appropriately thick cladding layers will be weakly confined and therefore have significant cavity loss.

The authors are grateful to H. F. Chung for crystal growth; D. Fork, G. Anderson, and F. Endicott for setting up the experiment; D. Sun, S. Ready, and J. Walker for processing assistance; and R. D. Bringans for his generous support. This work was financially supported by the United States Department of Commerce DoC Contract No. ATP-70NANB2H1241, and the Defense Advanced Research Projects Agency (DARPA Contract No. MDA972-95-3-008).

[1] S. Nakamura, M. Senoh, S. Nagahama, N. Iwasa, T. Yamada, T. Matsushita, H. Kiyoku, and Y. Sugimoto, Jpn. J. Appl. Phys. 1 **35**, L74 (1996).
[2] S. Nakamura, M. Senoh, S. Nagahama, N. Iwasa, T. Yamada, T. Matsushita, Y. Sugimoto, and H. Kiyoku, Appl. Phys. Lett. **69**, 1477 (1996).
[3] S. Nakamura, M. Senoh, S. Nagahama, N. Iwasa, T. Yamada, T. Matsushita, Y. Sugimoto, and H. Kiyoku, Appl. Phys. Lett. **69**, 1568 (1996).
[4] D. P. Bour, H. F. Chung, W. Götz, L. Romano, B. S. Krusor, F. A. Ponce, N. M. Johnson, and R. D. Bringans, *Characterization of AlGaInN Heterostructures grown by OMVPE*, Electrochemical Society Proceedings, 1996, Vol. 96-11, p. 37.
[5] H. Amano, T. Asahi, and I. Akasaki, Jpn. J. Appl. Phys. 1 **29**, L205 (1990).
[6] H. Amano, T. Tanaka, Y. Kunii, S. T. Kim, and I. Akasaki, Appl. Phys. Lett. **64**, 1377 (1994).
[7] X. H. Yang, T. J. Schmidt, W. Shan, J. J. Song, and B. Goldenberg, Appl. Phys. Lett. **66**, 1 (1995).
[8] T. J. Schmidt, X. H. Yang, W. Shan, J. J. Song, A. Salvador, W. Kim, Ö. Aktas, A. Botchkarev, and H. Morkoç, Appl. Phys. Lett. **68**, 1820 (1996).
[9] H. Yonezu, I. Sakuma, K. Kobayashi, T. Kamejima, M. Ueno, and Y. Nannichi, Jpn. J. Appl. Phys. **12**, 1585 (1973).
[10] J. C. Dyment, Appl. Phys. Lett. **10**, 84 (1967).
[11] Z. L. Liau, R. L. Aggarwal, P. A. Maki, R. J. Molnar, J. N. Walpole, R. C. Williamson, and I. Melngailis, Appl. Phys. Lett. **69**, 1665 (1996).
[12] V. J. Masin and G. A. Evans, User's manual of program MODEIG/II for Macintosh (1987).
[13] I. Akasaki (private communication, 1995).